

Modeling of an autonomous microgrid for renewable energy sources integration

Serban, I.; Teodorescu, Remus; Guerrero, Josep M.; Marinescu, C.

Published in:

Industrial Electronics, 2009. IECON '09. 35th Annual Conference of IEEE

DOI (link to publication from Publisher):

[10.1109/IECON.2009.5414923](https://doi.org/10.1109/IECON.2009.5414923)

Publication date:

2009

Document Version

Publisher's PDF, also known as Version of record

[Link to publication from Aalborg University](#)

Citation for published version (APA):

Serban, I., Teodorescu, R., Guerrero, J. M., & Marinescu, C. (2009). Modeling of an autonomous microgrid for renewable energy sources integration. In *Industrial Electronics, 2009. IECON '09. 35th Annual Conference of IEEE* (pp. 4311-4316). IEEE (Institute of Electrical and Electronics Engineers).
<https://doi.org/10.1109/IECON.2009.5414923>

General rights

Copyright and moral rights for the publications made accessible in the public portal are retained by the authors and/or other copyright owners and it is a condition of accessing publications that users recognise and abide by the legal requirements associated with these rights.

- Users may download and print one copy of any publication from the public portal for the purpose of private study or research.
- You may not further distribute the material or use it for any profit-making activity or commercial gain
- You may freely distribute the URL identifying the publication in the public portal -

Take down policy

If you believe that this document breaches copyright please contact us at vbn@aub.aau.dk providing details, and we will remove access to the work immediately and investigate your claim.

Modeling of an Autonomous Microgrid for Renewable Energy Sources Integration

I. Serban¹, R. Teodorescu², J. M. Guerrero³, and C. Marinescu¹

1. Transilvania University of Brasov, Romania

2. Institute of Energy Technology, Aalborg University, Denmark

3. Technical University of Catalonia, Spain.

ioan.serban@unitbv.ro, ret@iet.aau.dk, josep.m.guerrero@upc.edu, corneliu.marinescu@unitbv.ro

Abstract- The frequency stability analysis in an autonomous microgrid (MG) with renewable energy sources (RES) is a continuously studied issue. This paper presents an original method for modeling an autonomous MG with a battery energy storage system (BESS) and a wind power plant (WPP), with the purpose of frequency stability analysis. A reduced order model is developed, considering only the dominant elements in the frequency control loop.

The model's parameters are identified from experimental results, and the presented results are focused on frequency response for variable load and variable wind speed.

I. INTRODUCTION

The developing of hybrid power systems with renewable energy sources (RES) represents a new step towards distributed generation. These systems are often grouped into single-phase and three-phase micro-grids (MG) and supply mostly domestic loads in remote areas. A typical MG contains several energy sources and consumers, operating as one entity, and producing electric and sometimes thermal energy. Controlling such a MG involves the use of interfacing, protective and control elements for each generator, and devices to regulate the voltage and frequency.

A MG can operate autonomously or interconnected with the public grid. In autonomous operating mode, the generating units should share the active and reactive power in the MG, and they have to maintain the stability of the system. The control problem of autonomous MGs is a continuous debating subject [1]-[3], mainly regarding the frequency stability. In an autonomous MG with RES, predominating wind power, power balance is difficult to achieve, mainly because of the wind power variations, difficult to predict. An efficient way to overcome this problem is to use an energy storage system that acts as a buffer between the generators and loads. The energy storage system can be implemented with various type of batteries [4]-[6], fuel cells [7], or combination of both [8].

Modeling an autonomous MG has become an important stage in the system developing process and the literature abounds with methods for this purpose. The models can have different complexities depending of the modeling goal. Simplified models can be used for analysis of the electromechanical parts and frequency stability where the time constants involved in frequency response are much larger than other electrical time constants [9]. Full-order

models are used for analyzing small-signal stability in systems with high penetration of fast-acting power electronics converters [10].

The paper aims to develop a model of an autonomous MG with a battery energy storage system (BESS) and a wind power plant (WPP) for analyzing the frequency stability, in certain operating conditions.

The paper is organized as follows: in Section II the system configuration is presented, Section III describes the modeling of the MG components, Section IV analyzes the model applied on an experimental MG and the conclusions are provided in Section V.

II. SYSTEM CONFIGURATION

The studied system, presented in Fig. 1, consists in a wind power plant (WPP) and a battery energy storage system (BESS), both connected on an AC single-phase microgrid (MG), operating in autonomous mode. The WPP is variable-speed with a multi-pole permanent magnet synchronous generator (PMSG) directly connected to the wind turbine (WT). A converter, consisting in a diode rectifier, a DC-bus and an inverter, accomplishes the interface between the generator and MG. The inverter injects active power at unity power factor, without any voltage or frequency control on the point of common coupling.

The BESS ensures the power balance in the MG, acting as a load or as a source (generator) according to the sign of power unbalance. Neglecting the power losses in the system, the active power balance is:

$$P_{BESS} = P_L - P_{WPP} \quad (1)$$

where: P_{BESS} is the BESS power (positive or negative), P_L is the load power, and P_{WPP} is the WPP power.

The active power balance must be ensured at any moment, in order to maintain the system's frequency within the required limits ($\pm 1\%$). The main sources of disturbances are the WPP, which injects variable active power according to the wind speed, and the loads that vary quasi-randomly.

Different strategies for maintaining the active power balance are used, based on energy storage, dump load control, or combination of both and load shedding.

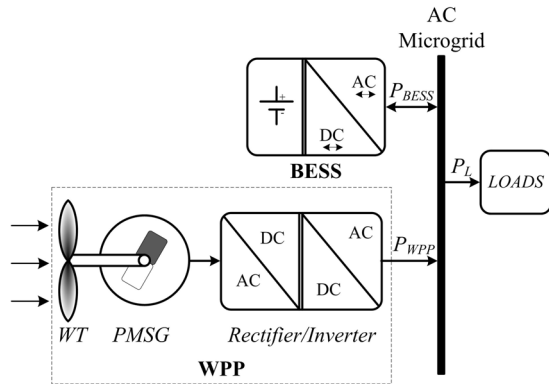


Fig. 1. MG system configuration

This paper focuses on the analysis of system dynamic response for different operating conditions, as variable wind speed or variable load power. The idea is to develop a simple and correct model of the microgrid from Fig. 1.

III. MG COMPONENTS MODELING

A. BESS modeling

The BESS consist in a voltage-source inverter connected to the MG through a low-frequency transformer and a battery on the DC side. The inverter is voltage controlled and ensures bidirectional power transfer between the battery and MG. The stiffness of the inverter and battery link is high, ensuring fast power transfer between the battery and microgrid.

The BESS operation is critical for the MG operation. The main attention is the control of the BESS inverter, which requires a particular control strategy to maintain both the voltage and frequency stability.

The literature presents various control schemes for such inverters and they are divided mainly in two solutions. The first one consists in measuring the system frequency and control real power [11]-[13]. The other solution, to measure the power and control the output frequency [14]-[15], is adopted in this paper too.

The basic of the BESS inverter control structure derives from the synchronous generator principle of operation. The active power balance in the system gives the frequency deviation while the reactive power flow influences the MG voltage. Both active and reactive power control loops are decoupled and they can be separately analyzed [16]-[18]. In this paper, it is adopted a simple and reliable control algorithm presented in Fig. 2, patented under the name *SelfSynchTM* [19]. The active and reactive powers are calculated from the voltage and current at the inverter output terminals [20] and they feed back the control loop.

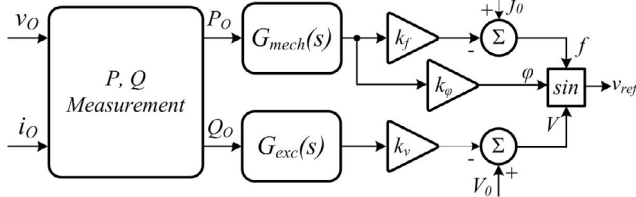


Fig. 2. SelfSynchTM algorithm

The calculated P and Q supply two first-order filters [$G_{mech}(s)$ and $G_{exc}(s)$] with time constants T_{mech} and T_{exc} , which mimics the mechanical moment of inertia and excitation time constants of a synchronous generator. These filters are introduced to decouple the active and reactive power control loops during transients, which are more rapid than one voltage cycle. They are also necessary for keeping the voltage and frequency constants in case of nonlinear loads. The values of time constants are a compromise between the inverter overload capacity and the requested smoothing effect in case of nonlinear loads mainly [19].

The second section of the control structure allows the inverter to operate in droop mode, in multi-master microgrid architectures. In this mode, two or more inverters with voltage and frequency control capability can share the power without using high-speed communication networks [18]. Another aspect of this section is the phase feed-forward which has a major impact on the system's stability over a wide range [16]. The parameter K_ϕ is negative having a damping effect, and its value is chosen according to the system's architecture and the number of parallel inverters [19].

The output of the block form Fig. 2 is the reference voltage for the inverter, which is driven by two cascaded voltage and current control loops [17].

We are interested only in the frequency stability of the microgrid, so we will neglect the effect of the internal voltage and current control loop, and it will be considered that the voltage is in steady state regardless the active power variations. Therefore, only the active power – frequency control path from Fig. 2 will be taken into account in our model. The frequency/active power transfer function of the BESS will be represented as follows:

$$G_{BESS}(s) = \frac{\Delta f}{\Delta P_{BESS}} = (K_f + sK_\phi) \cdot G_{mech}(s) \quad (2)$$

where:

$$G_{mech}(s) = \frac{1}{1 + sT_{mech}} \quad (3)$$

From these equations results:

$$G_{BESS}(s) = \frac{K_f + sK_\phi}{1 + sT_{mech}} \quad (4)$$

In the following, the active powers will be in per units and the base power is P_{BESS} .

B. WPP modeling

1. Aerodynamic model

The amount of mechanical power captured from wind by a three-blade wind turbine can be expressed as [21]:

$$P_m = \frac{\rho}{2} c_p(\lambda, \beta) A v_w^3 \quad (5)$$

where: ρ is the mass density of air [kg/m³]; A is the blades' swept area [m²]; v_w is the velocity of the wind [m/s]; $c_p(\lambda, \beta)$ is the power coefficient of the wind turbine; λ is tip

speed ratio of the rotor blade tip speed to wind speed; β is the blades pitch angle [deg].

The wind turbine considered is passive stall controlled, so $\beta=0$ and the tower shadow and wind shear effects are neglected.

The WPP is interfaced with the MG by a current controlled PWM inverter, which injects power at unity power factor. The mainly used control strategies for grid-connected inverters are presented in [22]. The inverter response is very fast relative to the other time constants in the WPP dynamics and therefore it will be modeled as a simple power amplifier.

The injected power into the grid depends linearly of the DC bus, being defined a minimum and a maximum DC voltage. These values correspond to zero and the rated power of the inverter. The characteristic of the DC bus voltage function of the WTG rotor speed can be approximated by a linear function estimated from experimental measurements. Therefore, the following relation expresses the relationship between the WPP power and WT rotor speed in the linear region, in per unit:

$$P_{WPP}(\omega_r) = \frac{\omega - \omega_{\min}}{1 - \omega_{\min}}, \quad \omega = [\omega_{\min} \dots 1] \text{p.u.} \quad (6)$$

where: ω_{\min} is the minimum rotor speed when the WPP begin to produce power.

Fig. 3 shows the wind turbine characteristics function of rotor speed for different wind speeds, and the steady-state operating curve based on (6). Fig. 4 shows the characteristic curve of the WPP output power versus wind speed, which will be used hereinafter for the WPP model.

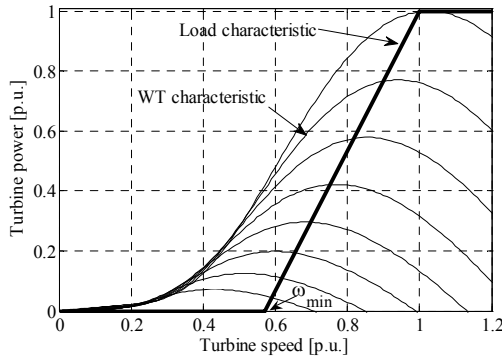


Fig. 3. Wind Turbine characteristics and steady-state operating curve

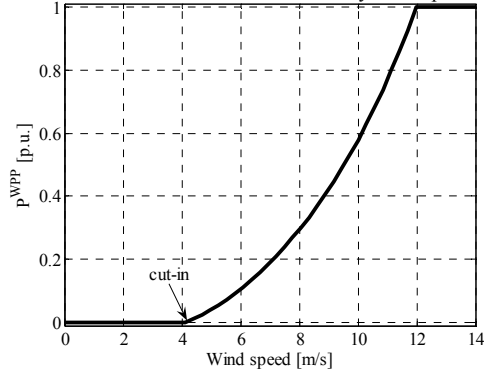


Fig. 4. WPP output power versus wind speed

2. Small-signal wind turbine model

The wind turbine is a nonlinear element in the WPP model and its characteristics depends of the wind speed and rotor speed. For small-signal modeling purpose the characteristic can be linearised in different steady-state operating points, by using the following expression:

$$\Delta P_m = K_{\omega} \cdot \Delta \omega_r + K_w \cdot \Delta v_w \quad (7)$$

where: K_{ω} and K_w are the partial derivatives of the mechanical power, as follows:

$$K_{\omega} = \left. \frac{\partial P_m}{\partial \omega_r} \right|_{v_w=ct} \quad \text{and} \quad K_w = \left. \frac{\partial P_m}{\partial v_w} \right|_{\omega_r=ct} \quad (8)$$

Table I form Appendix presents the values of K_{ω} and K_w for wind speeds between 5 and 12m/s.

The dynamics of the WPP involves mechanical and electrical time constants. The wind turbine is directly connected with the PMSG by a rigid shaft and therefore a one-mass equivalent model of the mechanical drive train will be considered. The model is described by the following equation of motion in per unit, where for small deviations it may be used power instead of torques [23]:

$$\Delta P_m - \Delta P_e = 2H \frac{d\Delta \omega_r}{dt} \quad (9)$$

where: ΔP_m is the mechanical power; ΔP_e is the electrical power of the PMSG; ω_r is the angular velocity of the common shaft; H is the combined inertia constant of the wind turbine and generator.

The speed/mechanical power transfer function is expressed as:

$$G_m(s) = \frac{\Delta \omega_r}{\Delta P_m} = \frac{1}{2H \cdot s} \quad (10)$$

The dynamic behavior of the PMSG – electrical converter power path is considered a first order lag, as given next:

$$G_e(s) = \frac{\Delta P_e}{\Delta \omega_r} = \frac{K_e}{1 + \tau_e \cdot s} \quad (11)$$

where: K_e is the amplification factor in per unit and depends of the wind turbine rated power; τ_e is the time delay between the wind turbine speed change and the electrical power injected into the grid by the inverter.

The first order filter acts as a decoupling element between the wind turbine and the grid-side inverter and in this study the inverter control scheme does not include any other decoupling element between the DC-bus and grid power.

3. PLL model

The electronically interfaced generators are much faster than conventional rotating machines and they do not have the

capability of storing energy during transients [24]. While in a conventional rotating machine, the mechanical inertia of the rotor influences the frequency stability, in an electronically interfaced generator the main source of oscillations is the PLL (Phase Locked Loop) [25]. It ensures the synchronization of the inverter voltage with the grid voltage. Proper selection of its parameters ensures good system stability. Under variable voltage, phase or frequency, the PLL will require a certain time for resynchronization. The PLL linearised model can be expressed by the following transfer function [26]:

$$G_{PLL}(s) = \frac{sK_p^{PLL} + K_I^{PLL}}{s^2 + sK_p^{PLL} + K_I^{PLL}} \quad (12)$$

where K_p^{PLL} and K_I^{PLL} are the parameters of the internal proportional-integral (PI) filter.

Approximating the active power of the inverter directly proportional with its power angle:

$$P_{WPP} = \frac{V_{MG}V_{WPP}}{X_{WPP}} \cong K_\theta \cdot \theta \quad (13)$$

where: $K_\theta = P_n/\theta_n$ is the ratio between the rated power and power angle and $\theta = \delta_{MG} - \delta_{WPP}$, the difference between the MG voltage angle and WPP inverter voltage angle; X_{WPP} is the coupling reactance of the WPP inverter to the MG.

From (11)-(13) we can write the expression of the output WPP power as follows:

$$\Delta P_{WPP} = \Delta P_e - K_\theta \cdot \frac{s}{s^2 + sK_p^{PLL} + K_I^{PLL}} \cdot \Delta f \quad (14)$$

The WPP is modeled by the following expression:

$$\Delta P_{WPP} = \Delta f \cdot G_f^{WPP}(s) + \Delta v_w \cdot G_w^{WPP}(s) \quad (16)$$

where:

$$G_f^{WPP}(s) = \frac{\Delta P_{WPP}}{\Delta f} = -K_\theta \cdot \frac{s}{s^2 + sK_p^{PLL} + K_I^{PLL}} \quad (17)$$

and

$$G_w^{WPP}(s) = \frac{\Delta P_{WPP}}{\Delta v_w} = \frac{K_w K_e}{2H \tau_e \cdot s^2 + (2H - K_w \tau_e) \cdot s + K_e - K_\omega} \quad (18)$$

C. Overall system model

The model has two inputs, one is the load power deviation and the other is the wind speed. The loads are considered independent with small frequency variations as most of the domestic loads.

The system is modeled by the following expression:

$$\Delta f = \Delta P_L \cdot G_1(s) + \Delta v_w \cdot G_2(s) \quad (19)$$

where:

$$G_1(s) = \frac{\Delta f}{\Delta P_L} = \frac{G_{BESS}}{1 + G_{BESS} \cdot G_f^{WPP}} \quad (20)$$

$$G_2(s) = \frac{\Delta f}{\Delta v_w} = -\frac{G_{BESS} \cdot G_w^{WPP}}{1 + G_{BESS} \cdot G_f^{WPP}} \quad (21)$$

IV. SYSTEM ANALYSIS

A. Identification of model's parameters

To identify the parameters involved in the proposed model several tests were carried out on an experimentally microgrid with the structure form Fig. 1, at the Institute of Energy Technology from Aalborg, Denmark. The BESS is a 5kW SunnyIsland™ type commercial inverter with a standard 48V lead-acid battery bank on the DC side. The WPP consist in a 1.5kW wind turbine connected to a 1.7kW WindyBoy™ type commercial inverter.

The system has been tested for variable load and power from the WPP and the frequency variation was recorded for analysis, with a power analyzer. The employed parameters of the model have been calculated with the system identification technique and they are listed in Table I, in Appendix.

B. Results and discussion

In this section, the model outlined previously is verified for different operating conditions. The results are divided in three parts: load power variation, wind speed variation and analysis of the microgrid stability when several identical WPP are connected in parallel.

1. Load Step without and with WPP connected

To perform this analysis, the frequency response of the MG for a 1 p.u. step load connection is illustrated in Fig. 5 in two conditions: without and with WPP connected in the microgrid. The frequency waveforms match very closely the experimental measurements with negligible error.

In the first case, the MG frequency variation is given only by the BESS, while in the second case the WPP influences the frequency response because of the internal PLL dynamic. It requires a certain time to resynchronize with the voltage phase and during this period, the phase WPP and BESS voltages are phase shifted, leading to transitory power flow from the WPP to the BESS. Fig. 6 presents the power variation for BESS and WPP. When the load power changes ($t = 1s$) the WPP injects power for a small period, until the PLL resynchronize with the voltage.

2. Variable wind speed

The wind speed variation is another perturbing factor in the MG, and this section presents the system behavior for 1% wind step, for different steady-state operating points, corresponding to 5, 8 and 12 m/s in wind speed. The 1% step in wind speed lead to WPP power variation and consequently the MG frequency is changing like in Fig. 7. For the three different operating points, the power-wind speed slope (K_w) has different values, given in Table I.

The presented model is useful for system stability analysis when one or more parameters are changing. On this line, it has been performed the stability analysis of the MG system for several operating points, and Fig. 8 presents the trajectory of two-pairs of complex-conjugate dominant poles when the wind speed changes from 5m/s to the nominal value of 12m/s. The oscillation frequency of the poles varies between 0.8 and 1 Hz approximately and they have a high damping with a damping factor of 0.9 to 0.98.

3. Analysis of the microgrid stability when more identical WPP are connected in parallel

The third studied aspect is the system stability when more identical WPP are connected in parallel on the MG. Fig. 9 shows the trajectory of the low-frequency dominant poles when n_{WPP} varies from 1 to 10, for similar operating conditions. When the number of WPP increases, the dominant poles become less damped and the oscillation frequency decreases from 0.8Hz to 0.6Hz. This effect can be observed also in Fig. 10, which presents the frequency response for 1 p.u. load power step for $n_{WPP} = 1, 5$ and 10. Of course, in practice, depending of the application, when the number of wind turbines increases it has to be considered to add more power in the BESS or to use more BESS in parallel, and consequently the parameters K_ϕ from (4) will change, increasing the damping in the system.

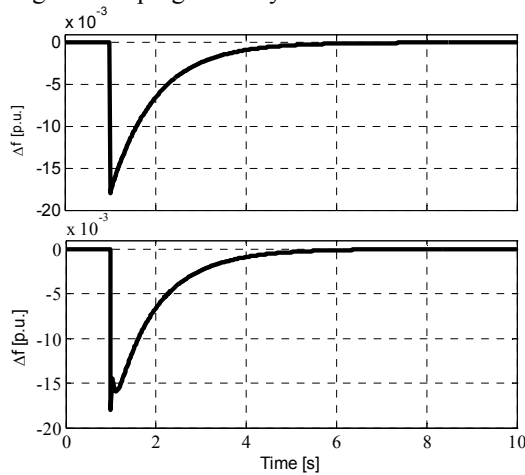


Fig.5. Frequency deviation for 1 p.u. load step (without and with WPP)

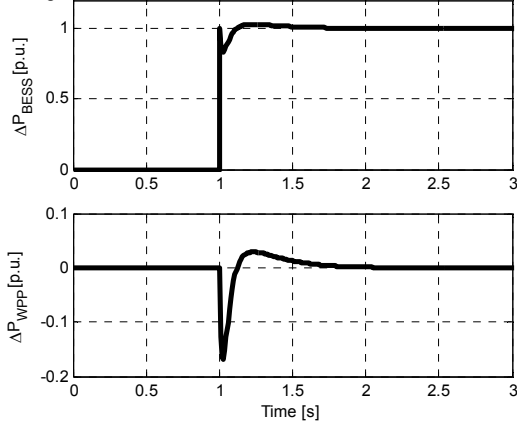


Fig.6 BESS and WPP active power for 1 p.u. load step

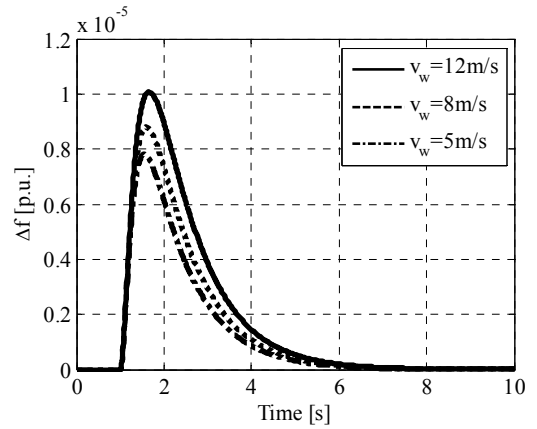


Fig.7 Frequency deviation for 1% wind speed increase

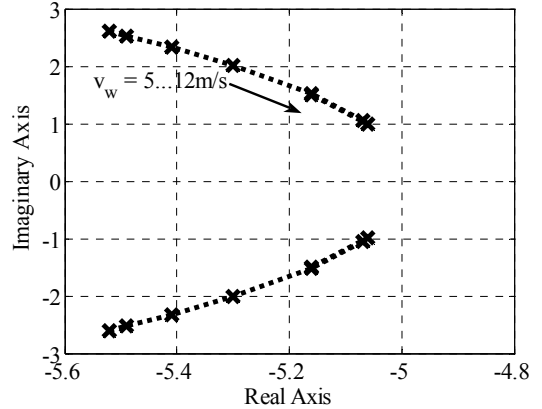


Fig.8. Trace of dominant poles for various wind speeds

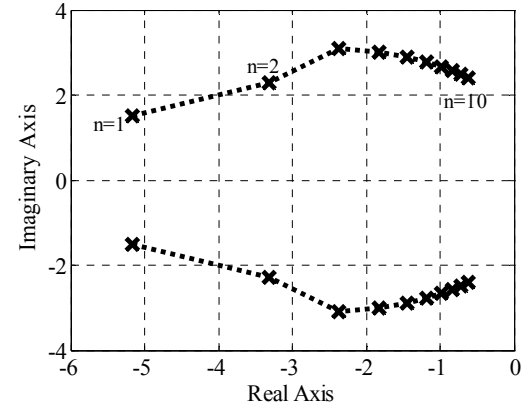


Fig.9 Trace of dominant poles when connecting several WPP in parallel

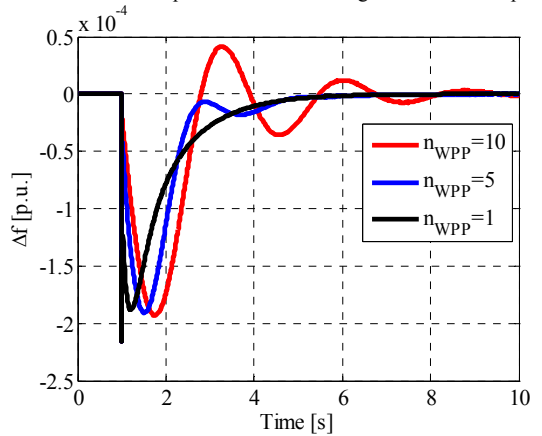


Fig.10. Frequency deviation for 1 p.u. load step for several WPP in parallel

V. CONCLUSIONS

The paper has presented a method for modeling an autonomous microgrid (MG) for frequency stability analysis. The MG consists in a wind power plant (WPP) along with a battery energy storage system (BESS). The BESS performs the voltage and frequency control, while the WPP injects active power into the grid at unity power factor. The model took into account only the dominant elements of the system, which are involved in the MG frequency control, thus reducing the complexity of the model. This aspect is considered very important in complex systems.

The presented results are focused on the dynamic frequency response for variable load and variable wind speed. The MG stability is analyzed for various operating conditions and dynamic frequency change has been compared when more identical WPP are connected in parallel. It has been proven that when the number of WPP increases the dominant poles become less damped leading to frequency oscillations. The solution of this problem is to add more BESS, increasing the damping of the system.

The model is very helpful for further studies in the analysis of the frequency behavior in autonomous microgrids.

ACKNOWLEDGMENT

This research theme is supported in part by the project CNCISIS IDEI 134/2007, financed by The Romanian Ministry of Education Research and Innovation.

REFERENCES

- [1] T. Senjyu, T. Nakaji, K. Uezato, and T. Funabashi, "A Hybrid Power System Using Alternative Energy Facilities in Isolated Island", *IEEE Trans. Energy Conversion*, vol. 20, no. 2, pp.406-414, June 2005.
- [2] P. Piagi, and R. H. Lasseter, "Autonomous Control of Microgrids", *IEEE PES Meeting*, Montreal, June 2006.
- [3] J.A. Pecos Lopes, C.L. Moreira, and A.G. Madureira, "Defining Control Strategies for MicroGrids Islanded Operation", *Trans. Power Systems*, vol. 21, no. 2, pp. 916-924, May 2006.
- [4] R. Sebastian, and J. Quesada, "Distributed Control System for Frequency Control in a Isolated Wind System", *Science-Direct – Renewable Energy*, vol.31, issue 3, pp. 285-305, March 2006.
- [5] B. Singh, G. Kasal, A. Chandra, and Kamal-Al-Haddad, "Battery Based Voltage and Frequency Controller for Parallel Operated Isolated Asynchronous Generators", *IEEE International Symposium on Industrial Electronics*, pp. 883-888, June 2007, Vigo, Spain.
- [6] L. Barote, R. Weissbach, R. Teodorescu, C. Marinescu, and M. Cirstea, "Stand-Alone Wind System with Vanadium Redox Battery Energy Storage", *Proceedings of the 11th International Conference on Optimization of Electrical and Electronic Equipment*, vol II-B, pp. 407-412, 22-23May 2008, Brasov, Romania.
- [7] T. Senjyu, T. Nakaji, K. Uezato, and T. Funabashi, "A Hybrid Power System Using Alternative Energy Facilities in Isolated Island", *IEEE Trans. Energy Conversion*, vol.20, no.2, pp.406-414, June 2005.
- [8] D.J. Lee, and L. Wang, "Small-Signal Stability Analysis of an Autonomous Hybrid Renewable Energy Power Generation/Energy Storage System Part I: Time-Domain Simulations", *IEEE Trans. Energy Conversion*, vol.23, no.1, pp.311-320, March 2008.
- [9] E. Ortjohann, W. Sinsukthavorn, A. Mohd, N. Hamsic, A. Schmelter, and D. Morton, "Modeling/Simulation of Power Distribution in Hybrid Power Systems Using Dynamic RMS-Technique", *Proceedings of the International Conference on Power Engineering, Energy and Electrical Drives- POWERENG 2007*, pp. 779-784, April 2007, Setubal, Portugal.
- [10] N. Pogaku, M. Prodanovic, and T.C. Green, "Modeling, Analysis and Testing of Autonomous Operation of an Inverter-Based Microgrid", *IEEE Trans. Power Electronics*, vol. 22, pp. 613-625, March 2007.
- [11] I. Serban, and C. Marinescu, "Power Quality Issues in a Stand-Alone Microgrid Based on Renewable Energy", *Revue Roumaine des Sciences Techniques.– Électrotechn. et Énerg.*, vol. 53(3), pp. 285-293, June-September 2008.
- [12] F. Katiraei, and M.R. Iravani, "Power Management Strategies for a Microgrid With Multiple Distributed Generation Units", *IEEE Trans. Power Systems*, vol. 21, no.4, pp. 1821-1831, November 2006.
- [13] I. Serban, C.P. Ion, and C. Marinescu, "Frequency Control and Unbalances Compensation in Stand-Alone Fixed-Speed Wind Turbine Systems", *Proceedings of the 34th Annual Conference of the IEEE Industrial Electronics Society–IECON'08*, pp. 2167-2172, November 2008, Florida, USA.
- [14] A. Engler, C. Hardt, P. Strauß, and M. Vandenbergh, "Parallel Operation of Generators for Stand-Alone Single-Phase Hybrid Systems", *EPVSEC*, October 2001, Munich.
- [15] J.M. Guerrero, J. Matas, L. Garcia, M. Castilla, and J. Miret, "Wireless-Control Strategy for Parallel Operation of Distributed-Generation Inverters", *IEEE Trans. Industrial Electronics*, vol.53, no.5, pp. 1461-1470, October 2006.
- [16] A. Engler, O. Osika, M. Barnes, N. Jenkins, and A. Arulampalam "Large Scale Integration of Micro-Generation to Low Voltage Grids", *European project, Contract no. ENK-CT-2002-00610*, February 2004.
- [17] B. Burger, P. Zacharias, G. Cramer, and W. Kleinkauf, "Inverters for Modular and Extendable Electric Energy Supply Systems", *Use of Electronic-Based Power Conversion for Distributed and Renewable Energy Sources*, Institute fur Solare Energieversorgungstechnik, 2008.
- [18] A. Engler, "Applicability of Droops in Low Voltage Grids", *International Journal of Distributed Energy Resources*, vol.1, no.1, pp.3, January - March 2005.
- [19] A. Engler, US Patent No.: US 6,693,809 B2, Feb. 2004.
- [20] B. Burger, and A. Engler: "Fast Signal Conditioning in Single Phase Systems", *Proceedings of the 9th European Conference on Power Electronics and Applications –EPE*, 2001.
- [21] Siegfried Heier, "Grid Integration of Wind Energy Conversion Systems – second edition", John Wiley & Sons Ltd, USA, 2006.
- [22] F. Blaabjerg, R. Teodorescu, M. Liserre, and A. V. Timbus, "Overview of Control and Grid Synchronization for Distributed Power Generation Systems", *IEEE Trans. Industrial Electronics*, vol. 53, no. 5, pp. 1398-1409, Oct. 2006.
- [23] I. Boldea, "Synchronous Generators – The Electric Generators Handbook", CRC Press, USA, 2006.
- [24] P. Piagi, "Microgrid Control", Ph. D Thesis, Electrical Engineering Department, University of Wisconsin-Madison, Aug. 2005.
- [25] F. Katiraei, M.R. Iravani, and P.W. Lehn, "Small-signal dynamic model of a micro-grid including conventional and electronically interfaced distributed resources", *IET generation, transmission & distribution*, vol.1, no.3, pp. 369-378, May 2007.
- [26] Se-Kyo Chung, "A Phase Tracking System for Three Phase Utility Interface Inverters", *IEEE Trans. Power Electronics*, vol.15, no.3, pp.431-438, May 2000.

APPENDIX

TABLE I
PARAMETERS OF THE SYSTEM

BESS		WPP
$P_{BESS} = 5 \text{ kW}$		$P_{WPP} = 1.5 \text{ kW}$
$T_{mech} = 1 \text{ s}$		$K_e = 1.5/5$
$K_f = 0 \text{ Hz/Wp.u.}$		$H = 0.2 \text{ s}$
$K_\phi = -5.65 \text{ rad/Wp.u.}$		$\omega_{min} = 0.57 \text{ p.u.}$
		$\tau_\phi = 0.06 \text{ s}$
		$K_p = 65, K_i = 1500$
		$K_\theta = 11.5 \text{ Wp.u./rad}$
WT small-signal model parameters		
v_w [m/s]	K_ω [Wp.u./rad]	K_w [Wp.u./m.s ⁻¹]
5	-0.32	0.063
8	-0.1189	0.1208
10	0.08404	0.167
12	0.00325	0.2501